Reflection FWI from fully deghosted towed-streamer data: A field data example

Jaime Ramos-Martinez, Kathy Zou, Steve Kelly, and Boris Tsimelzon, PGS*

Summary

Success in the application of gradient-based full-waveform inversion (FWI) depends on the extraction of the lowest possible wavenumber content provided by the data. In shallow water scenarios with shallow targets, the refractions and diving waves present in the large offsets of streamer data provide an advantageous framework for such success. In deep water scenarios with streamer data containing only reflections, the extraction of the long wavelength features requires either a boost in the low-frequency content of the data and/or strategies to precondition the data and the model to reduce the nonlinearity of the problem. In this work, we invert reflection events from fully deghosted streamer data that were acquired in deep water offshore of Norway. The deghosting was accomplished by using dual-sensor streamers and a time and depth-distributed source array. The inverted velocity model shows a significant improvement in resolution in the shallow part of the model, which consequently improves the resolution of the migrated image. Results are also validated by the flatness of common image gathers and the waveform fitting between modeled and field shot records.

Introduction

In recent years, several field data examples have demonstrated the successful application of FWI (Tarantola, 1984) for improving the resolution of both velocity models and migrated images (e.g., Sirgue et al., 2009; Barkved et al., 2010; Liu et al., 2012). Most of these examples were acquired in shallow water, and they demonstrated improvement for shallow targets, typically by using OBC recordings. The reason for this has been broadly discussed (e.g., Vireux and Operto 2009). FWI depends on the success of extracting the lowest wavenumber content from the data. This is achieved by using the lowest frequency content of data with coherent signals, and by recording the longest possible offsets in order to take advantage of the refracted and diving waves. When data are acquired with conventional streamer acquisition, the reliability of the inverted models thus depends on the presence of refracted or diving waves.

In deep water scenarios, it is very likely that only reflections are present in towed streamer data. This exacerbates the need for special acquisition strategies that satisfy the requirements discussed above. In the same context, innovative strategies are needed for preconditioning the inversion in order to extract long-wavelength features. Acquisition-based methods have recently been proposed in order to improve the low-frequency part of the spectrum (e.g., Farouki et al., 2011; Moldoveanu et al., 2012). In addition, several strategies have been proposed in order to retrieve the long wavelength features of the velocity models within the FWI framework (e.g., Kelly et al., 2010; Xu et al., 2012; Zhou et al., 2012).

In this work, we show a successful example of FWI using a dataset acquired with dual-sensor, streamer recording and a time and depth-varying source array. The data used for inversion are free of source and receiver ghosts. They exhibit coherent signals at frequencies below 3Hz. The water column is about 1.3 km deep, so only reflected events are present in the data. The results show significant improvement in the resolution of the velocity model and therefore in the migrated image. We also use the quality of the waveform fitting between the modeled and recorded data, as well as the flatness of common image gathers, as QC tools in order to validate the inversion results.

Data Preconditioning

The dataset was acquired in the Møre Margin area in the Norwegian Sea using dual-sensor streamers at 25 m depth, and a time and depth-distributed source at 10 m and 14 m depths, with a maximum offset of 10050 m. The implementation of this source array with the use of dual-sensor streamers allows full deghosting of the data. Hegna and Parkes (2012) provide a detailed description of the benefits of eliminating acquisition-related effects in order to improve data bandwidth.

Preprocessing steps applied to this 2D dataset before FWI include noise-attenuation, source and receiver-side deghosting, and multiple attenuation. In Figure 1, we show samples of shot records after the preprocessing and filtering with two different bandwidths that have corner frequencies of 1, 2, 5 and 10 Hz [panel (a)], and 1, 2, 3, and 6 Hz [panel (b)]. The corresponding spectra are shown in panel (c). The comparison shows that there are coherent reflected events at frequencies lower than 3 Hz. We used the data with broader bandwidth for inversion.

We normalized the modeled data with respect to the field data using the water bottom reflection. This normalization was performed by implicitly including the effect of the density contrast at the water bottom. A mute was then

DOI http://dx.doi.org/10.1190/segam2013-1333.1

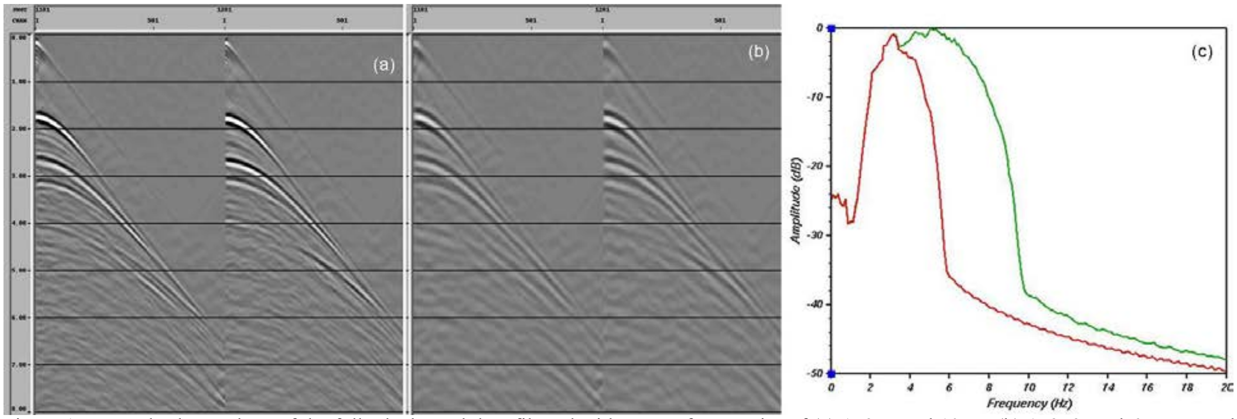

Figure 1: Example shot gathers of the fully deghosted data filtered with corner frequencies of (a) 1, 2, 5 and 10 Hz (b) 1, 2, 3, and 6 Hz. Panel (c) shows the amplitude spectra of the data in (a) and (b) in green and red curves, respectively.

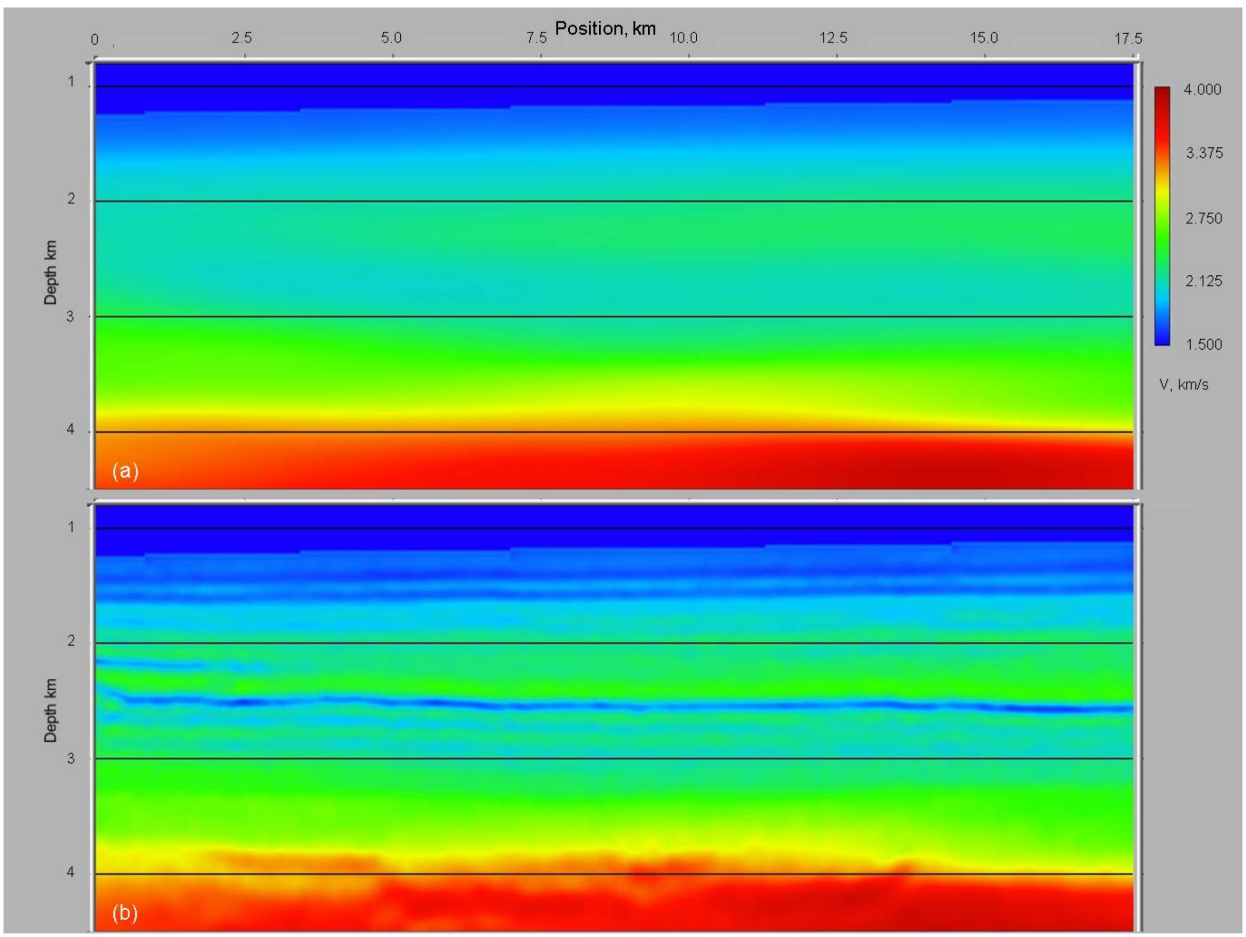

Figure 2: (a) Starting model for the inversion. (b) Inverted velocity model.

DOI http://dx.doi.org/10.1190/segam2013-1333.1

applied just below the water bottom reflection in order to exclude it from the inversion, while retaining as many post-critical events as possible.

Inversion Results

We applied a gradient-based inversion algorithm that is implemented in the time domain. Synthetic wavefields were computed by solving the scalar wave equation using the pseudo-analytic method (Etgen and Brandsberg-Dhal, 2009). Although the algorithm is capable of handling anisotropy, we obtained good results assuming isotropy. We applied the formulation of Tarantola (1984), which uses the spatial distribution of the back-propagated data residual for updating the velocity model. Figure 2a shows the starting velocity model, which was obtained from velocities used in pre-stack time domain migration. Figure 2b shows the inverted velocity model after 10 iterations, which exhibits a much higher resolution than the starting model, down to a depth of 3 km.. Likewise, as shown in Figure 3, the inverted model shows a significant improvement in the waveform fitting between the modeled and recorded data after inversion.

To validate the inversion results, we used a Kirchhoff algorithm to compute Pre-Stack Depth Migrated (PSDM) gathers and stacked images. Figures 4a and 4b show common image gathers for the starting and inverted velocity models, respectively. The figures show that the overall improvement in the flatness of the gathers is significant. Figures 5a and 5b show migrated, stacked images, before and after the inversion, respectively. The resolution of the image is significantly improved by the inversion, down to a depth of 3 km. Improving the resolution of the deeper part of the velocity model is an on-going project, which may incorporate an integrated form of the reflectivity (impedance) in order to update the velocity model (Kelly et al., 2010) in a layer-stripping fashion.

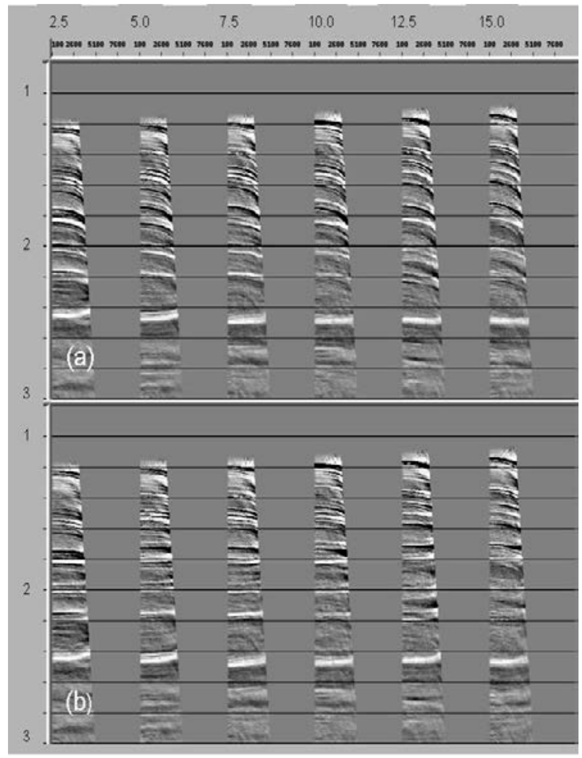

Figure 4: (a) Kirchhoff PSDM common image gathers with (a) the starting model and (b) the inverted model. The horizontal and vertical axes are lateral location and depth in km, respectively.

Conclusions

We have demonstrated the application of FWI using reflections in a deep-water environment. This was achieved by using ghost-free data with coherent signal at frequencies below 3Hz. The data were acquired with dual sensor towed-streamer and a time and depth variable source array. The inversion results show a significant

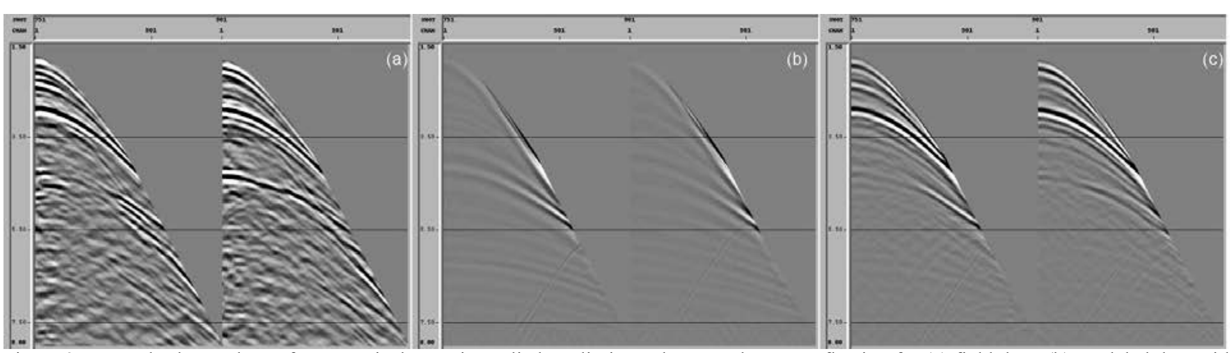

Figure 3: Example shot gathers after a surgical mute is applied to eliminate the water bottom reflection for (a) field data, (b) modeled data with the starting model, and (c) modeled data with the inverted model.

improvement in the resolution of both the velocity model and associated migrated images. The flatness of the image gathers and the improvement in waveform fitting between synthetic and field data demonstrate the accuracy of the inversion.

Acknowledgments

We acknowledge the contributions of Li Jiang and Peter Aaron at the initial stage of this work. We thank PGS Multiclient for providing the dataset. We thank Alejandro Valenciano, Nizar Chemingui and Sverre Brandsberg-Dahl for helpful discussions and suggestions, and Stephen Pharez for reviewing the abstract. Finally, we thank PGS for granting the authorization to publish this paper.

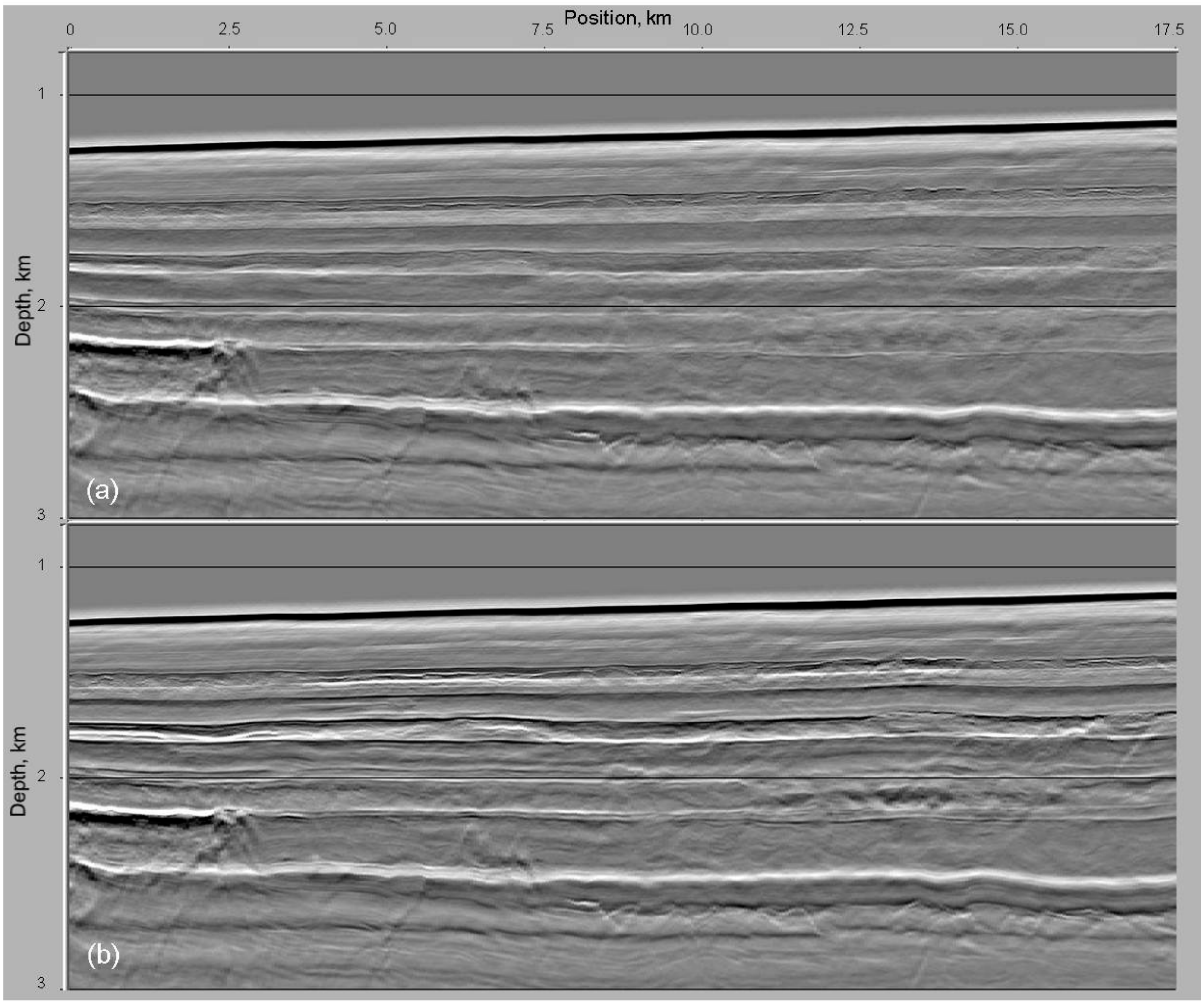

Figure 5: (a) Kirchhoff migrated images with (a) the starting model and (b) the inverted model. The stratigraphy of the sediments is better defined in the image with the FWI model.

DOI http://dx.doi.org/10.1190/segam2013-1333.1

http://dx.doi.org/10.1190/segam2013-1333.1

EDITED REFERENCES

Note: This reference list is a copy-edited version of the reference list submitted by the author. Reference lists for the 2013 SEG Technical Program Expanded Abstracts have been copy edited so that references provided with the online metadata for each paper will achieve a high degree of linking to cited sources that appear on the Web.

REFERENCES

Barkved, O., U. Albertin, P. Heavey, J. H. Kommedal, J. P. van Hestel, R. Synnove, H. Pettersen, and C. Kent, 2010, Business impact of FWI at Vallhal: 80th Annual International Meeting, SEG, Expanded Abstracts, 925–929.

Etgen, J., and S. Brandsberg-Dahl, 2009, The pseudo-analytical method: Application of pseudo-Laplacians to acoustic and acoustic anisotropic wave propagation: 79th Annual International Meeting, SEG, Expanded Abstracts, 2552–2555.

Farouki, M., A. Long, G. Parkes, and S. Hegna, 2011, Broadband towed marine seismic via total source and receiver de-ghosting: Proceedings of the SEGJ, International Symposium.

Hegna, S., and G. Parkes, 2012, The principle of using complementary acquisition components to achieve broadband seismic: Presented at the 82nd Annual International Meeting, SEG.

Kelly, S., J. Ramos-Martínez, B. Tsimelzon, and S. Crawley, 2010, Application of an impedance-based full-waveform inversion method for dual-sensor, single-streamer field recordings: Presented at the 72nd Annual International Conference and Exhibition, EAGE.

Liu, F., L. Guash, S. A. Morton, M. Warner, A. Umpleby, Z. Men, S. Fairhead, and S. Chekles, 2012, 3D time-domain full waveform inversion of a Valhall OBC dataset: Presented at the 82nd Annual International Meeting, SEG.

Moldoveanu, N., N. Seymour, D. J. Mannen, and P. Caprioli, 2012, Broadband seismic methods for towed-streamer acquisition: Presented at the 74th Annual International Conference and Exhibition, EAGE.

Sirgue, L., and O. J. Barkved, J.P., Van Gestel, O.J., Askim and J.H. Kommedal, 2009, 3D waveform inversion on Valhall wide-azimuth OBC: Presented at the 71st Annual International Conference and Exhibition, EAGE.

Tarantola, A., 1984, Inversion of seismic reflection data in the acoustic approximation: Geophysics, **49**, 1259–1266, http://dx.doi.org/10.1190/1.1441754.

Vireaux, J., and S. Operto, 2009, An overview of full-waveform inversion in exploration geophysics: Geophysics, **74**, no. 6, WCC1–WCC26, http://dx.doi.org/10.1190/1.3238367.

Xu, S., D. Wang, F. Chen, G. Lambare, and Y. Zhang, 2012, Inversion on reflected seismic wave: Presented at the 82nd Annual International Meeting, SEG.

Zhou, H., L. Amundsen, and G. Zhang, 2012, Fundamental issues in full-waveform inversion: Presented at the 82nd Annual International Meeting, SEG.